DEUTSCHES ELEKTRONEN-SYNCHROTRON **DESY**

DESY 88-067
ITP-UH 4/88
May 1988

NONSTANDARD PRODUCTION OF THE STANDARD HIGGS

by

B. Lampe, N. Vlachos

Institute für Theoretische Physik, Universität Hannover

ISSN 0418-9833

NOTKESTRASSE 85 · 2 HAMBURG 52

To be sure that your preprints are promptly included in the
HIGH ENERGY PHYSICS INDEX ,
send them to the following address (if possible by air mail) :

DESY
Bibliothek
Notkestrasse 85
2 Hamburg 52
Germany

DESY 88-067
ITP-UH 4/88
May 1988

ISSN 0418-9833

Nonstandard Production of the Standard Higgs

B. Lampe and N. Vlachos*
Institute of Theoretical Physics
University of Hannover
Appelstraße 2, 3000 Hannover, W-Germany

Abstract:
New interactions beyond the Fermi scale can be systematically studied in an effective Lagrangian approach. We have examined the contribution of all $SU_3 \times SU_2 \times U_1$ invariant effective operators of dimension six containing the Higgs field to the Higgsproduction rates in e^+e^-, ep and $p\bar{p}$ collisions and in toponium decay. Restrictions from low energy phenomenology on the strength of these operators are also discussed.

1. Introduction

The standard model of strong and electroweak interactions has been very successful phenomenologically. Among the particles of the standard model, however, least is known about the Higgs field. In fact it has not been observed so far. Theoretical production rates are small in general and detection seems difficult [1, 8, 11, 19].

In this work we assume that the standard model interactions of the Higgs field have to be supplemented by an additional exotic interaction with a characteristic energy scale Λ of the order of 1 TeV. At energies below Λ a systematic and model independent way to describe such phenomena is by means of an effective Lagrangian approach. The total Lagrangian is written as an expansion in powers of $1/\Lambda$.

* supported by DFG

$$\mathcal{L}_{eff} = \mathcal{L}_{SM} + \frac{1}{\Lambda}\mathcal{L}_1 + \frac{1}{\Lambda^2}\mathcal{L}_2 + \ldots . \qquad (1)$$

with L_{SM} the standard model Lagrangian.

Two conditions are imposed upon the L_i

- the L_i have the same field content as L_{SM}
- the L_i have the same symmetries as L_{SM}.

In particular one assumes all L_i to be $SU_3 \times SU_2 \times U_1$- invariant, since the $SU_2 \times U_1$ symmetry is restored for energies above the Fermiscale. These assumptions imply $L_1 = 0$, so that the analysis should centre around the dimension six operators in L_2. In [2, 3] all possible contributions to L_2 have been collected. For many of the operators physical consequences have been discussed [4]. In this work we are going to concentrate on terms containing the Higgs field, because it is conceivable that nonstandard effects will show up first in interactions of the Higgs particle. Note that eq.(1) should only be taken as a generic expression. L_2 is not the sum of all possible dimension six interactions, but a definite linear combination of them with most of the coefficients vanishing. We shall even restrict ourselves to the case that L_2 consists of only one operator at a time, so that mutual interferences among different operators can be neglected. Interference with the standard model is taken into account, however.

The organization of this article is as follows: In section 2 we review Higgs production in the standard model. We only list the nonnegligible processes. For many other possible production mechanisms the standard model cross sections are small. For them the general philosophy that Λ-effects are very small as compared to the standard model is no longer true. In sections 3 and 4 the exotic interactions are analysed. Some of them contain higher powers of the Higgs doublet Φ. In the

physical gauge, $\varphi = \begin{pmatrix} 0 \\ v+H \end{pmatrix}$ with v = 174 GeV and H the physical Higgs field. Therefore contributions linear in H always exist . The cross sections found are to be compared with the standard model results in order to determine the value of Λ for which the exotic contributions begin to dominate. Operators, which are severely restricted by low energy phenomonology are not taken into account. Such restrictions are usually to be applied on terms generated by the background term $|_{H=0}$.

In the first parts of the paper we shall tacitly pursue a scenario, in which 30 GeV $\lesssim m_H \lesssim$ 300 GeV, although formally the results are true for any value of m_H.

2. Higgs Production in the Standard Model

When talking about Higgs production in this and the following section, we actually mean single Higgs production . In the standard model there are only two vertices containing one Higgs field. They are shown in fig. 1. Among them the Higgs-fermion interaction is suppressed by a factor m_f/v and can be neglected for the light fermions. Therefore in order to produce a Higgs at an appreciable rate one needs a (real or virtual) W, Z or t to start with.

a) If $m_H < 2m_t$, Wilczek [5] suggested that the Higgs particle could be produced in the radiative decay of toponium $\Theta \to H\gamma$ (c.f. fig. 2). He found for the decay rate in the nonrelativistic quark model

$$\frac{\Gamma(\Theta \to H\gamma)}{\Gamma(\Theta \to \mu^+\mu^-)} = \frac{1}{2\pi\alpha} \frac{m_t^2}{2v^2} \left(1 - \frac{m_H^2}{4m_t^2}\right) \qquad (2)$$

This formula was further improved [6] and the signatures of the decay were worked out in detail [7] . The process can be identified rather uniquely because of the monochromatic photon. Note that, if $m_t > m_Z$, Θ would predominantly decay via the weak interaction, thereby depleting the branching ratio for $\Theta \to H\gamma$.

b) The dominant production mechanism at LEP is shown in fig. 3. The integrated cross section for this process is [8]

$$\sigma = \frac{2m_Z^4}{v^2} \frac{\alpha(v_e^2 + a_e^2)}{\sin^2\Theta_W \cos^2\Theta_W} \frac{\Delta(\Delta^2/4s + 3m_Z^2)}{12 s m_Z^2 (s - m_Z^2)^2} \qquad (3)$$

Here $v_e = \frac{1}{4} - \sin^2\Theta_W$ and $a_e = \frac{1}{4}$ are the Z-charges of the electron. Δ is the usual invariant for a 2 → 2 scattering process,

$$\Delta^2 = m_H^4 + m_Z^4 + s^2 - 2s m_H^2 - 2s m_Z^2 - 2 m_H^2 m_Z^2 \qquad (4)$$

It is related to the c.m. momentum p of the Higgs via

$$p = \frac{\Delta}{2\sqrt{s}} \qquad (5)$$

Equation (3) is written in such a way that the contribution from the Higgs-vertex becomes explicit. The result is drawn in fig. 4 where it is needed as a comparison with nonstandard contributions. It peaks at $\sqrt{s} = m_Z + \sqrt{2}m_H$ and, above threshold, is by no means small. The asymptotic limit of (3) is $\sigma = 0.445 \cdot 10^{-3}/s$.

c) At the $p\bar{p}$ collider one may have bremsstrahlung off a Z, just as in fig. 3, as well as bremsstrahlung off a W. However at present energies the rate from this process is significantly smaller than the cross section for the so called gluon fusion mechanism [5], which is depicted in fig. 5. For convenience we shall neglect lighter fermions, such as the

b-quark, running in the loop. The cross section can be thought as being derived from an effective Higgs-gluon interaction of the form

$$\mathcal{L}_{Hg} = \frac{N}{6 m_t} \frac{m_t}{\sqrt{2}\, v} \frac{\alpha_s(m_H^2)}{2\pi} G^a_{\mu\nu} G^{\mu\nu a} H \qquad (6)$$

where $G_{\mu\nu}$ is the gluon field strength and N is a function of m_H/m_t which is close to 1 if $m_t \geq 0.2\, m_H$ [11]. N assumes its maximum value 1.82 at $m_H/m_t \cong 2.5$.

Let us summarize: For Higgs masses $m_H < 2m_t$ ($<2m_Z$) the toponium system is an ideal H-factory. Because of the gluon fusion mechanism the $p\bar{p}$ collider is also a H-factory. However, it is plagued by background problems. Only for $m_H > 2m_Z$, when the Higgs particle decays predominantly into W and Z pairs, detection is unambiguous. In the intermediate mass range $2m_t < m_H < 2m_Z$ it is best to look at LEP. At very high energies (above 5 TeV) heavy vector boson fusion (fig. 9) becomes the most important contribution to the production cross sections [9].

For HERA no efficient production mechanism exists: Even at energies above 1 TeV (where heavy vector boson fusion dominates) the detection of the Higgs in ep reactions looks quite difficult [9].

In this section we did not discuss production mechanisms with negligible cross sections or with too strong background problems. Some of these get large contributions from exotic vertices and will be discussed in section 3.

3. Nonstandard Higgs Production

In this section we are going to examine all standard model invariant dimension six interactions and their possible contribution to Higgs production rates. These operators have

been systematically constructed in refs. [2, 3]. There exist six generic classes of operators containing the Higgs field. Besides H they contain either vector bosons V_μ (with field strenths $V_{\mu\nu}$ and covariant derivations D_μ) or fermions f or both.

A) $$\Omega^V := \frac{1}{2}(\varphi^+\varphi)\, V_{\mu\nu} V^{\mu\nu} \qquad (7)$$

In the physical gauge the relevant interaction is

$$\pm \frac{v}{\Lambda^2} H\, V_{\mu\nu} V^{\mu\nu} \qquad (8)$$

Similar operators involving dual field strengths exist and will be discussed later.

There ist no low energy restriction for the gluonic Ω^g, since $\Omega^g|_{H=0}$ can be absorbed into a strong coupling constant redefinition. Ω^g induces a gluon fusion process whose strength v/Λ^2 can be directly compared with the standard model contribution (6). The exotic interaction dominates the standard model for values of Λ up to 2.8 TeV.

The photon operator is of particular interest, since it allows the Higgs to decay directly into two photons. SU_2-invariance requires the existence of two operators, Ω^B and Ω^W, containing the photon. Here B denotes the U_1- and W the SU_2-gauge field. Unfortunately a general linear combination of them destroys the universality in charged and neutral currents and changes the ρ-parameter [2]. Only a very special linear combination, namely $\Omega^B + \Omega^W$, avoids these problems.

Events with two hard photons would simplify Higgs detection quite a lot. The standard model decay rate is small [1, 11], since it is proportional to α^2. The Higgs-photon coupling under consideration is of the form (8) corresponding to the vertex rule

$$-2i \frac{v}{\Lambda^2} (p_1 p_2 g_{\rho\sigma} - p_{1\rho} p_{2\sigma}) \qquad (9)$$

where $p_{1\sigma}$ and $p_{2\rho}$ are the momenta of the outgoing photons. Therefore the exotic decay rate is

$$\Gamma(H \xrightarrow{\Omega} \gamma\gamma) = \frac{v^2 m_H^3}{8\pi \Lambda^4} \qquad (10)$$

This result predicts a large branching ratio in the intermediate mass range $2m_t < m_H < 2m_W$, the region where we had difficulties detecting the Higgs in $p\bar{p}$ collisions in section 2. In that mass range the standard model Higgs decay is dominated by [1]*

$$\Gamma(H \to t\bar{t}) = \frac{m_H}{8\pi} \frac{m_t^2}{2v^2} \left(1 - \frac{4m_t^2}{m_H^2}\right)^{3/2} \qquad (11)$$

In fig. 6 the branching ratio is drawn as a function of m_H/m_Z for several values of $\Lambda(\tilde{\Lambda} := 2\Lambda)$. The branching ratio is very sensitive to Λ because of the quartic power of Λ in eq. (10).

* The decay $H \to gg$ is neglected here, because $\Gamma(H \to gg)/\Gamma(H \to t\bar{t})$ is small, if m_H is not too cloose to $2m_t$.

On the production side there are several interesting new mechanisms. However these mechanisms generally yield rather small cross sections, because one has to produce one or two photons introducing thereby powers of α and then one has a factor v^2/Λ^4 from the Higgs-photon vertex, so that one ends up with small quantities.
In ep collisions for example one has the process fig. 7, which seems interesting at first sight. Application of the Weizsäcker-Williams approximation [13], which is well suited to this process, shows however that at energies below one TeV the cross section is as small as the standard model contribution and therefore negligible.

In e^+e^- and $p\bar{p}$ collisions one has an interesting new production mechanism, namely the diagramm in fig. 3 with the Z replaced by a photon. There is also a Z-contribution from $\Omega^B + \Omega^W$, which is to be considered later. The total cross section for the process $e^+e^- \to H\gamma$ is given by

$$\sigma(e^+e^- \xrightarrow{\Omega} H\gamma) = \frac{8}{3}\alpha \frac{v^2}{\Lambda^4} \left(1 - \frac{m_H^2}{s}\right)^3 \qquad (12)$$

For m_H^2 far away from s the cross section only depends on Λ. In this case for $\Lambda = 1$ TeV it is $4.5\ 10^{-37}\text{cm}^2$ and for $\Lambda = 0.5$ TeV it is $3.5\ 10^{-36}\text{cm}^2$. For a LEP luminosity of $1\text{pb}^{-1}\text{day}^{-1}$ this is just at the edge of observability. One may reverse this statement by saying that existing (PETRA) data restrict Λ by $\Lambda > (1 - m_H^2/s)^{3/4}$ TeV.

Ω_B and Ω_W both contain a $H - \gamma - Z$ interaction, which for $m_H < M_Z$ would make the decay of a real Z into $H\gamma$ possible.

(In the standard model this decay rate is negligible [14].) In the sum $\Omega_B + \Omega_W$ the H - γ - Z interaction drops out, so we are not going to consider it.

Let us now calculate the Ω-contribution to $e^+e^- \to HZ$. The total cross section can be written with the help of the same quantities as eq. (3). It is

$$\sigma(e^+e^- \xrightarrow{\Omega,SM} HZ) = \frac{\alpha(v_e^2+a_e^2)\Delta}{\sin^2\Theta_W\cos^2\Theta_W(s-m_Z^2)^4}\left\{\frac{\Delta^2+12sm_Z^2}{24sv^2}m_Z^2\right.$$

$$\left. + m_Z^2\,\frac{m_Z^2+s-m_H^2}{\sqrt{2}\Lambda^2 s} + v^2\,\frac{\Delta^2+6sm_Z^2}{6s\Lambda^4}\right\} \qquad (13)$$

The second term inside the curly bracket is the interference of the standard model and the exotic interaction. In fig. 4 we have drawn the total cross section as a function of $\sqrt{s}$ for two values of m_H and for Λ = 0.8 TeV. One can see that for such a value of Λ the Ω-contribution may be unraveled at LEP II.

B) $$\tilde{\Omega} := (\varphi^+\varphi)\, V_{\mu\nu}\,\tilde{V}^{\mu\nu} \qquad (14)$$

The gluon version of $\tilde{\Omega}$ contradicts the neutron electric dipole moment bounds [12]. Therefore we concentrate on the electroweak versions. The other qualitative difference as compared to Ω is the possibility of a HγZ-interaction, so that in addition to the decay mode $H \to \gamma\gamma$ also $H \to \gamma Z$ is possible. One can get the width for the former decay simply by replacing Λ by $\tilde{\Lambda}/2$ in equation (10), so that the numerical results are those of fig. 6. If in addition a factor $(1-m_Z^2/m_H^2)^3$ is added, one gets the width for $H \to \gamma Z$:

$$\tilde{\Gamma} = \frac{2v^2m_H^3}{\pi\tilde{\Lambda}^4}\,(1-m_Z^2/m_H^2)^3 \qquad (15)$$

The operator containing the H γ Z-interaction also predicts real Z decay with width $\tilde{\Gamma}(m_H \leftrightarrow m_Z)$. Comparing this to the standard model total decay width of the Z, $\Gamma_Z \approx 2.3$ GeV, we find a branching ratio of

$$BR(Z \to H\gamma) \approx 0.006\,(1\,\mathrm{TeV}/\tilde{\Lambda})^4\,(1-m_H^2/m_Z^2)^3 \qquad (16)$$

which, for $\tilde{\Lambda} < 0.5$ TeV and m_H not to close to m_Z, should be observable.

Let us now consider the process $e^+e^- \longrightarrow H\gamma$ via a virtual Z boson. If $\tilde{\Omega}$ is to be a $SU_2 \times U_1$-invariant operator, $V_{\mu\nu}$ is a specific linear combination $\tau_\gamma A_{\mu\nu} + \tau_Z Z_{\mu\nu}$ of the photon and the Z boson field stength with $\tau_{\gamma,Z}$ depending on the Weinberg angle. If V is the U_1 gauge field, for example, then $\tau_\gamma = \cos^2\Theta_W$ and $\tau_Z = 2\sin\Theta_W\cos\Theta_W$. Taking into account also the effect of a virtual photon one gets the total cross section

$$\sigma(e^+e^- \xrightarrow{\tilde{\Omega}} H\gamma) = 16\alpha\,\frac{v^2}{\tilde{\Lambda}^4}\,(1-\frac{m_H^2}{s})^3\left\{\left[\tau_\gamma + \frac{v_e\tau_Z}{\sin\Theta_W\cos\Theta_W(1-\frac{m_Z^2}{s})}\right]^2 + \frac{\tau_Z^2a_e^2}{\sin^2\Theta_W\cos^2\Theta_W(1-m_Z^2/s)^2}\right\} \qquad (17)$$

This result yields somewhat larger cross sections than the corresponding equation (12) for Ω.

C) $$\Psi := (\varphi^+\varphi)(D_\mu\varphi^+)(D^\mu\varphi) \qquad (18)$$

There is a similar operator, $(\varphi^+ D^\mu\varphi)(D_\mu\varphi^+\varphi)$, which has problems with the ρ-parameter [2]. Therefore it will not be considered. Eq. (18) contains an interaction term connecting the Higgs field and two heavy vector bosons. This term has the same structure as the standard model interaction between heavy vector bosons and the Higgs-field because it comes from the ordinary kinetic term.
Therefore it induces the same production mechanisms, with a much smaller coupling strength, however. The strength of the exotic vertex dominates the standard model only for Λ up to 300 GeV. For Λ = 500, 700, 1000 GeV the exotic contribution is 34%, 17% and 8% of the standard model contribution respectively.

D) $$\Gamma_f := (\varphi^+\varphi)(\varphi\,\bar{F}_L\,f_R) + c.c. \qquad (19)$$

where F_L is an SU_2-doublet of fermions containing f_L.
One can get a bound on Γ_f by demanding that the (Yukawa) Higgs mechanism be the dominant source of mass. The most stringent bound comes from the electron, $\Lambda_e > 100$ TeV. The situation is acceptable for the bottom quark ($\Lambda_b > 1.1$ TeV) and the top quark. For these reasons we shall concentrate on Γ_t.
There is a contribution to toponium decay (if $m_H < 2m_t$), which one can get by replacing $\frac{m_t^2}{2v^2}$ in (2) by $\left(\frac{m_t}{\sqrt{2}v} + \frac{v^2}{\Lambda_t^2}\right)^2$.

The exotic contribution is equal to the standard model one at a ("critical") value of $\Lambda = v\sqrt{\sqrt{2}\,v/m_t}$, which is 386 GeV for m_t = 50 GeV and 498 GeV for m_t = 30 GeV.

E) $$\Sigma := \varphi\,\bar{F}_L\,\sigma_{\mu\nu}\,V^{\mu\nu}\,f_R + c.c. \qquad (20)$$

In the case of leptons $V_{\mu\nu}$ cannot contain the photon field strengh, because such a term would induce inacceptable large magnetic moments.

Such a restriction should not be relevant for toponium decaying into $H+\gamma$. The vertex rule is shown in fig. 10 and gives the decay rate

$$\frac{\Gamma(\theta \xrightarrow{\Sigma,SM} H\gamma)}{\Gamma(\theta \xrightarrow{SM} \mu^+\mu^-)} = \left[\frac{e\,Q_t}{\sqrt{2}\,v\,m_t\left(1-\frac{m_H^2}{4m_t^2}\right)} + \frac{2}{\Lambda^2}\right]^2 \frac{m_t^4\left(1-\frac{m_H^2}{4m_t^2}\right)^3}{8\pi^2\alpha^2\,Q_t^2} \qquad (21)$$

Note that the exotic contribution is enhanced by a heavy top quark, in contrast to the result for the operator Γ_t.
In table 1 we give the ratios of the exotic and standard model decay contributions for several values of m_H and m_t and $\Lambda = 0.4$ TeV.

Next, we examine the production mechanism via ep experiments (fig. 11). We calculated the cross secion in the Weizsäcker-Williams (WW) approximation [13]. The photon

is treated as quasi real, i.e. its density as coming out of the electron approximated by a function

$$P_\gamma(\eta) = \frac{\alpha}{2\pi} \frac{1+(1-\eta)^2}{\eta} \qquad (22)$$

where η is the fraction of the electron energy carried away by the photon. P_γ is nothing else than the "Altarelli-Parisi" kernel of quantum electrodynamics. Note that any heavy vector boson component in Σ is neglected a priori in the WW approximation.

For the WW approximation one needs the matrix element squared of the process depicted in fig. 8 ,

$$|M|^2 = \frac{16}{\Lambda^4} \hat{s}\hat{t} \qquad (23)$$

Here $\hat{s} = (p'+k'')^2$ and $\hat{t} = (k''-p)^2$ are the usual $2 \longrightarrow 2$ invariants (on the parton level). Note that there is no singularity for $q^2 \longrightarrow 0$. Note also that we have neglected the interference with the standard model. This is justified, since the standard model contribution is very small.

Now we insert eq. (23) into the general formula for the total cross section in the WW approximation,

$$\sigma_{tot} = \int_{m_H^2/S}^{1} d\eta\, P_\gamma(\eta) \ln \frac{t_{max}}{t_{cut}} \int_{m_H^2/S}^{1} dx \sum_f q_f(x,P^2) Q_f^2 \int_{m_H^2-\hat{s}}^{0} d\hat{t}\, \frac{|M|^2}{64\pi \hat{s}^2} \qquad (24)$$

Here $\sqrt{S}$ is the total energy , $t_{max} = S - m_H^2$ and t_{cut} is a cutoff , which is chosen to be ≈ 1 GeV^2 [13]. q_f are the quark distribution functionswith Bjorken's x and $P^2 = (t_{max} - t_{cut})/\ln \frac{t_{max}}{t_{cut}}$ as variables.Here and in the following we are using the parametrization of the distribution functions given by Duke and Owens (set 1) [18]. In eq. (24) it

is understood that

$$\hat{s} = \eta \times S \qquad (25)$$

Results are drawn in fig. 12. At HERA ($\sqrt{S} \approx 300$ GeV) cross sections down to 0.1 pb may be measureable. We conclude that Σ might be accessible at HERA as long as

$$\Lambda < 1 \text{ TeV and } m_H < 50 \text{ GeV},$$

As far as the $p\bar{p}$ collider is concerned one may have a Higgs particle in conjunction with a prompt photon via the parton subprocess $q\bar{q} \longrightarrow H\gamma$. The cross section

$$\sigma(p\bar{p} \xrightarrow{\Sigma} H\gamma X) = \int_0^1 dx_1 \int_0^1 dx_2 \sum_f q_f(x_1,\hat{s})\, q_f(x_2,\hat{s})$$

$$\frac{\hat{s}}{3\pi\Lambda^4} \left(1 - \frac{m_H^2}{\hat{s}}\right)^3 \Theta(\hat{s} - m_H^2)\, \delta(x_1 x_2 S - \hat{s}) \qquad (26)$$

is orders of magnitude above the corresponding standard model one as long as $\Lambda < 2$ TeV. It is drawn in fig. 13 as a function of the $p\bar{p}$ energy for $\Lambda = 1$ TeV and two values of the Higgs mass.

One may ask whether existing collider data restict the value of Λ . The answer is yes. The prompt photon together with the decay products of the Higgs give so clear a signal that the experiments would have seen cross sections as small as 0.1 pb. (This number is only a very crude estimate, but remember that the cross section (26) goes like Λ^{-4}.) This implies $\Lambda > 1.5$ TeV for $m_H = 20$ GeV, $\Lambda > 1.3$ TeV for $m_H = 50$ GeV and $\Lambda > 1$ TeV for $m_H = 100$ GeV. From this we can conclude that the process in fig. 11 will not be seen at HERA.

The gluon version of Σ in $p\bar{p}$-collisions induces a mechanism

where the Higgs is produced along with a jet (c.f. fig. 14). The signature of such events is not as remarkable as for the $H\gamma$ events discussed in the last paragraph. However because of the large gluon density inside the proton the cross section is larger. Since the cross section formula is similar to (26), we do not give it here. We have drawn instead the cross section for Λ = 1 TeV and m_H = 50 and 100 GeV in fig. 15.

Again existing collider data restrict the value of Λ. Assuming this time the critical cross section to be 1pb, the bound one gets is $\Lambda > 1.3$ TeV for m_H = 20 GeV, $\Lambda > 1$ TeV for m_H = 50 GeV and $\Lambda > 0.7$ TeV for m_H = 100 GeV.

The Z-version of Σ contributes to the process $e^+e^- \to HZ$ with a cross section

$$\sigma(e^+e^- \xrightarrow{\Sigma} HZ) = \Delta \frac{\Delta^2 + 3 s m_Z^2}{24\pi \Lambda^4 s^2} \qquad (27)$$

which is drawn in fig. 4. This time there is no interference with the standard model. At high energies the ratio of the exotic and standard model contribution is

$$\frac{(27)}{(3)} \longrightarrow 93.6 \frac{s^2}{\Lambda^4} \qquad (28)$$

which, for $\Lambda = \sigma$ (1 TeV) and LEP I is a small number. On the other hand at LEP II it would be measurable.

F) $$\Delta := (\bar{F}_L f_R)\, D_\mu D^\nu \varphi \;+\; \text{c.c.} \qquad (29)$$

In principle one may consider an operator

$$\left[\alpha\, \bar{F}_L (D_\mu f_R) + \beta\, (D_\mu \bar{F}_L) f_R\right] D^\nu \varphi \;+\; \text{c.c.} \qquad (30)$$

with arbitrary α, β, which would be fully consistent with the assumptions stated in the introduction. By restricting ourselves to (29) we implicitly assume a certain left-right universality of derivative couplings.

Δ contains a $H\bar{f}f$ interaction and an interaction involving an additional heavy vector boson. The Feynman rules for these two interactions are given in fig. 16.

Let us start with the contribution of fig. 16a to toponium decay $\Theta \to H\gamma$. It is such that we effectively have a replacement

$$\frac{m_t^2}{2v^2} \longrightarrow \left(\frac{m_t}{\sqrt{2}v} + \frac{m_H^2}{\Lambda^2}\right)^2 \qquad (31)$$

in Wilczek's formula (2). Contrary to (21) the exotic contribution grows with m_H and not with m_t. For all reasonable values of the parameters m_t, m_H and Λ the exotic contribution to the decay rate is less than 1 % of the standard model contribution. The situation is worse than for Σ, because in contrast to (20) the exotic contribution is multiplied by the fine structure constant.

The $H\bar{f}f$ interaction has virtual effects on angular distributions in e^+e^-, ep and $p\bar{p}$ collisions. However for small couplings the general experience is that these effects are seen not much below H threshold [15]. The production cross section for $e^+e^- \to H$ is

$$\frac{\sigma(e^+e^- \xrightarrow{\Delta} H)}{\sigma(e^+e^- \xrightarrow{SM} H)} = 2\,\frac{v^2}{\Lambda^4}\,\frac{m_H^4}{m_e^2} \approx 2.32\cdot 10^{11}\left(\frac{m_H}{\Lambda}\right)^4 \qquad (32)$$

We have normalized to the standard model contribution, which is very small because of the small electron mass. Eq. (32) is a qualitatively new effect, as long as m_H is not too small and Λ not too large. E.g. for $m_H = 50$ GeV, $\Lambda = 1$ TeV the ratio is $1.43 \cdot 10^6$! Similarly the cross section for $p\bar{p} \to HX$ is much bigger than in the standard model [10] and given by

$$\sigma(p\bar{p} \xrightarrow{\Delta} HX) = \frac{\pi m_H^2}{6\Lambda^4} \sum_f \int_\tau^1 dx\,\frac{\tau}{x}\left[q_f(x,m_H^2)\,\bar{q}_f\left(\frac{\tau}{x},m_H^2\right) + (q \leftrightarrow \bar{q})\right] \qquad (33)$$

where $\tau = m_H^2/S$. It is drawn in fig. 17 as a function of $\sqrt{S}$ for $\Lambda = 1$ TeV and two values of m_H. It is a slowly varying function of $\sqrt{S}$ with typical values O(1pb). By comparison with existing e^+e^- and $p\bar{p}$ data one can in principle exclude values on the m_H-Λ-plane. These bounds do not come from virtual effects like the contribution to Bhabba scattering, because this is small of order Λ^{-8}. They come from direct detection analyses, in which no scalar particle giving the decay products of the Higgs was found. Let us assume for the e^+e^- process a critical cross section of 1pb. For the $p\bar{p}$ process it is much larger, because the decay products of the Higgs have to be disentangled from ordinary Drell Yan background. From the PETRA experiments one can then conclude $\Lambda > 0.3$ TeV for $m_H = 20$ GeV, $\Lambda > 0.5$ TeV for $m_H = 30$ GeV and $\Lambda > 0.7$ TeV for $m_H = 44$ GeV.

Δ gives also a contribution to $e^+e^- \to HZ$. The total cross section is

$$\sigma(e^+e^- \xrightarrow{\Delta} HZ) = \frac{\alpha\,\Delta^3}{32\Lambda^4 s\, m_Z^2 \sin^2\Theta_w \cos^2\Theta_w} \qquad (34)$$

Since the interference with the standard model vanishes, one can directly compare eqs. (3) and (34). For large s the ratio is

$$\frac{(34)}{(31)} \approx 2.89\,\frac{s^3}{m_Z^2\Lambda^4} \qquad (35)$$

For other values of s the cross section (34) can be found in fig. 4. Because of the factor α in (34) it is smaller than the corresponding contribution from Σ as long as the energy is not too large.

G) $$\Phi := i\,(\varphi^+ D_\mu \varphi)\,(\bar{f}\,\gamma^\mu f) \qquad (36)$$

where f may be either a left- or a righthanded fermion. Operators of this type violate the universality in weak and neutral currents [2]. Nevertheless some linear combination of them may escape the phenomenological and theoretical restrictions.

Concerning the field content Φ is very similar to the operator Δ, eq. (29). However the set of interesting production mechanisms is much more restricted, since in (36) neither the gluon nor the photon field appear. Also one can see easily that the process $f\bar{f} \xrightarrow{\Phi} H$ has a vanishing cross section. We conclude that it would be difficult to find effects of Φ in colliding beam experiments, if this operator should exist. Even the contributions to processes, which are nonnegligible in the standard model, are very small. For instance the contribution to the Wilczek mechanism of toponium decay is

$$\frac{\Gamma(\Theta \xrightarrow{\Phi} H\gamma)}{\Gamma(\Theta \xrightarrow{SM} H\gamma)} = \frac{2v^4}{\Lambda^4}\,(\alpha-\beta)^2 \qquad (37)$$

In eq. (37) we have taken for $\bar{f}\,\gamma_\mu f$ the general linear combination

$$\alpha\,\bar{t}_R\gamma_\mu t_R + \beta\,\bar{t}_L\gamma_\mu t_L .$$

4. Multiple Higgs Production

Two (or more) Higgses in the final state will give a rather clear experimental signal in the form of 4 jets or 4 leptons or 2 jets and 2 leptons. This holds for small Higgs mass; for larger values of m_H the signal will be even clearer, because one gets heavy quarks and/or heavy vector bosons.

In the standard model there is only one vertex involving more than one Higgs and another type of particle, namely an interaction of 2 Higgses with 2 heavy vector bosons. Its strength of $m^2_{W,Z}/v^2$ is by no means negligible. Therefore the process drawn in fig. 18 was examined [16], in order to determine whether the corresponding cross section is large enough to make itself observable at LEP. The net effect was found to be quite small, because there are too many rather heavy particles in the final state. One would rather have a photon instead of a Z in fig. 18a. This is the case for the photon version of the operator Ω, eq. (7). The problem here is the small couplings, which have already made the contribution to $e^+e^- \to H\gamma$ quite small (c.f. eq. (12)). We find

$$\frac{\sigma(e^+e^- \xrightarrow{\Omega} HH\gamma)}{\sigma(e^+e^- \xrightarrow{\Omega} H\gamma)} = \frac{s}{512\pi^2 v^2}\left(1 + \sigma(m_H^2/s)\right) \qquad (38)$$

Note the additional suprression factor $512\pi^2$ which is due to the fact that the three particle phase space is "smaller" than the two particle one. It is only at very high energies that double Higgs production is preferred to the single one.

Double Higgs production can also be obtained by gluon gluon fusion as described in the gluon version of Ω. The cross sections are given by

$$\sigma(p\bar{p} \xrightarrow{\Omega^g} HX) = \frac{\pi}{8}\tau \frac{v^2}{\Lambda^4} \int_\tau^1 \frac{dx}{x} F_g(x, m_H^2)\, F_g\left(\frac{\tau}{x}, m_H^2\right) \qquad (39)$$

and

$$\sigma(p\bar{p} \xrightarrow{\Omega^g} HHX) = \int_0^1 dx_1 \int_0^1 dx_2\, F_g(x_1, \hat{s})\, F_g(x_2, \hat{s})\, \hat{\sigma}(\hat{s})\, \delta(\hat{s} - x_1 x_2 S) \qquad (40)$$

where F_g is the gluon density and

$$\hat{\sigma}(\hat{s}) = \frac{\hat{s}}{32\pi\Lambda^4}\sqrt{1 - 4m_H^2/\hat{s}} \qquad (41)$$

is the parton cross section for $gg \xrightarrow{\Omega^g} HH$. Fig. 19 shows the result (40) as a function of $\sqrt{S}$ for $\Lambda = 1$ TeV and various values of the Higgs mass. Numbers for eq. (39) can be obtained by proper rescaling of the standard model result as given in the literature [17]. Due to phase space effects the double Higgs production rate is two or three orders of magnitude smaller than the single Higgs production rate. Nevertheless for Λ well below 1 TeV and not too large Higgs masses the process may be observable. Note that the numbers in fig. 19 gain a factor of 16, if one descends from $\Lambda = 1$ TeV to $\Lambda = 0.5$ TeV.

There are other operators involving higher powers of the Higgs field, cf. eqs. (18), (19) and (36). However within the framework of our discussion none of them qualifies as an interesting multiple Higgs production mechanism.

5. Conclusion

In this work we have investigated exotic Higgs interactions in a systematic and model independent way. We have concentrated on the real Higgs and did not consider virtual, i.e., indirect effects. Some of the interactions look exotic but due to $SU_3 \times SU_2 \times U_1$ invariance and low energy restrictions there are not as many qualitatively new features as expected. One of them is the direct Higgs-photon interaction, which leads to an interesting new decay channel for the Higgs particle. Another one is an interaction of the Higgs particle with light fermions which is very small in the standard model. This allows for very direct Higgs production mechanisms in e^+e^- and $p\bar{p}$ collisions.

In general the exotic effects are accessible only for characteristic scales Λ below 1 TeV. Among the Higgs-gauge-field interactions those with a gauge field strength are better off than those arising from a covariant derivative, since the latter involve the standard model coupling constants e,g,g' or g_s in front of the gauge-fields.

Table 2 provides a list which summarizes our results on the various operators on a qualitative level. If one is very optimistic, one may conclude that the different types of operators can be disentangled already by their qualitative properties. The difference between them is expected to be still more dominant in angular distributions. In this work we did not attempt to calculate any of them and concentrated on total cross sections. In this sense our paper is only a first step towards investigating exotic interactions of the Higgs boson.

There is one $p\bar{p}$ process which we did not consider in this paper, namely $gg \rightarrow t\bar{t}H$. This process may well be a good test on the operators Σ and Δ, in case they have a coupling proportional to the fermion mass (cf. the discussion in ref. [2]).

Acknowledgement

We acknowledge many discussions with W. Buchmüller.

References

[1] J. Ellis, M.K. Gaillard, D.V. Nanopoulos, Nucl. Phys. B106 (1976) 292
J.F. Gunion, Proceedings of the conference on search for scalar particles, Trieste 1987, eds. J.C. Pati, Q. Shafi
[2] W. Buchmüller, D. Wyler, Nucl. Phys. B268 (1986) 621
[3] C.J.C. Burges, H.J. Schnitzer, Nucl. Phys. B228 (1983) 464
C.N. Leung, S.T. Love, S. Rao, Z. Phys. C 31 (1986) 433
[4] E.J. Eichten, K.D. Lane, M.E. Peskin, Phys. Rev. Lett. 50 (1983) 811
R. Rückl, Phys. Lett. 129B (1983) 363
W. Buchmüller, B. Lampe, N. Vlachos, Phys. Lett. 197 (1987) 379
[5] F. Wilczek, Phys. Rev. Lett. 39 (1977) 1304
[6] J. Ellis, M.K. Gaillard, D.V. Nanopoulos, C.T. Sachrajda, Phys. Lett. 83B (1979) 339
M.J. Vysotsky, Phys. Lett. 97B (1980) 159
[7] A. Ali, G. Mikenberg, Z. Phys. C3 (1979) 147
[8] see, for example, E. Eichten, J. Hinchcliffe, K. Lane, C. Quigg, Rev. Mod. Phys. 56 (1984) 688 or H. Baer et al., Physics in LEP, CERN 86-02
[9] S. Midorikawa, M. Yoshimura, Nucl. Phys. 163B, (1980) 365
R.N. Cahn, S. Dawson, Phys. Lett. 136B (1984) 196
G.L. Kane, W.W. Repko, W.B. Rolnick, Phys. Lett. 148B (1984) 367
M.S. Chanowitz, M.K. Gaillard, Nucl. Phys. B261 (1985) 379
R.N. Cahn, Nucl. Phys. B255 (1985) 341
G. Altarelli, B. Mele, F. Pitolli, Nucl. Phys. B287 (1987) 205
[10] H.M. Georgi, S.L. Glashow, M.E. Machacek, D.V. Nanopoulos, Phys. Rev. Lett. 40 (1978) 692
[11] A.A. Ansel'm, N.G. Ural'tsev, V.A. Khoze, Sov. Phys. Usp. 28 (1985) 113
[12] V. Baluni, Phys. Rev. D19 (1979) 2227
[13] G. Altarelli, G. Martinelli, B. Mele, R. Rückl, Nucl. Phys. B262 (1985) 204
[14] R.N. Cahn, M.S. Chanowitz, N. Fleishon, Phys. Lett. 82B (1979) 113
[15] W. Hollik, B. u. F. Schrempp, Phys. Lett. 140B (1984) 424
[16] G.J. Gounaris, D. Schildknecht, F.M. Renard, Phys. Lett. 83B (1979) 191
[17] V.D. Barger, R.J.N. Philipps, Collider Physics, Addison-Wesley 1987
[18] D.W. Duke, J.F. Owens, Phys. Rev. D30 (1984) 49
[19] R. Cahn et al. and D.M. Atwood et al., in: Proceedings of the Workshop on Experiments, Detectors and Experimental Areas for the Supercollider, Berkeley 1987

Table 1 Ratios of the Σ-over the standard model toponium decay contributions to Higgs production for $\Lambda = 400$ GeV.

m_H	m_t	
20	50	69 %
20	80	119 %
40	80	106 %
50	200	287 %
80	200	256 %

Table 2 Qualitative effects of exotic operators

	toponium	e^+e^-	ep	$p\bar{p}$	decay
$\Omega = \frac{1}{2}(\varphi^+\varphi) V_{\mu\nu} V^{\mu\nu}$		x		x	x
$\Gamma = (\varphi^+\varphi)(\varphi \bar{F}_L f_R)$ + c.c.	x				
$\Sigma = \varphi \bar{F}_L \sigma_{\mu\nu} V^{\mu\nu} f_R$ + c.c.	x	x		x	
$\Delta = (\bar{F}_L f_R) D_\mu D^\mu \varphi$ + c.c.		x		x	

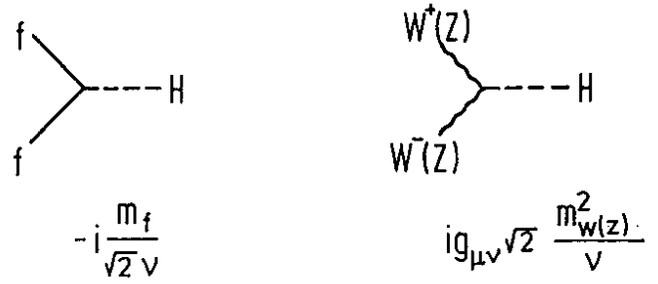

Fig. 1: Single-Higgs interactions in the standard model

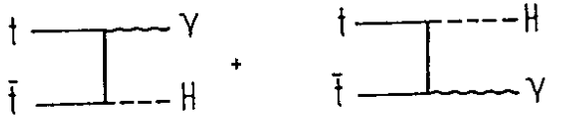

Fig. 2: Higgs production in toponium decay

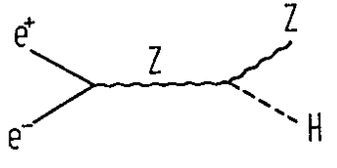

Fig. 3: Higgs production at LEP

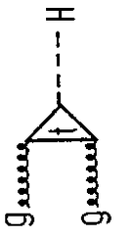

Fig. 5: Gluon fusion mechanism in $p\bar{p}$ collisions

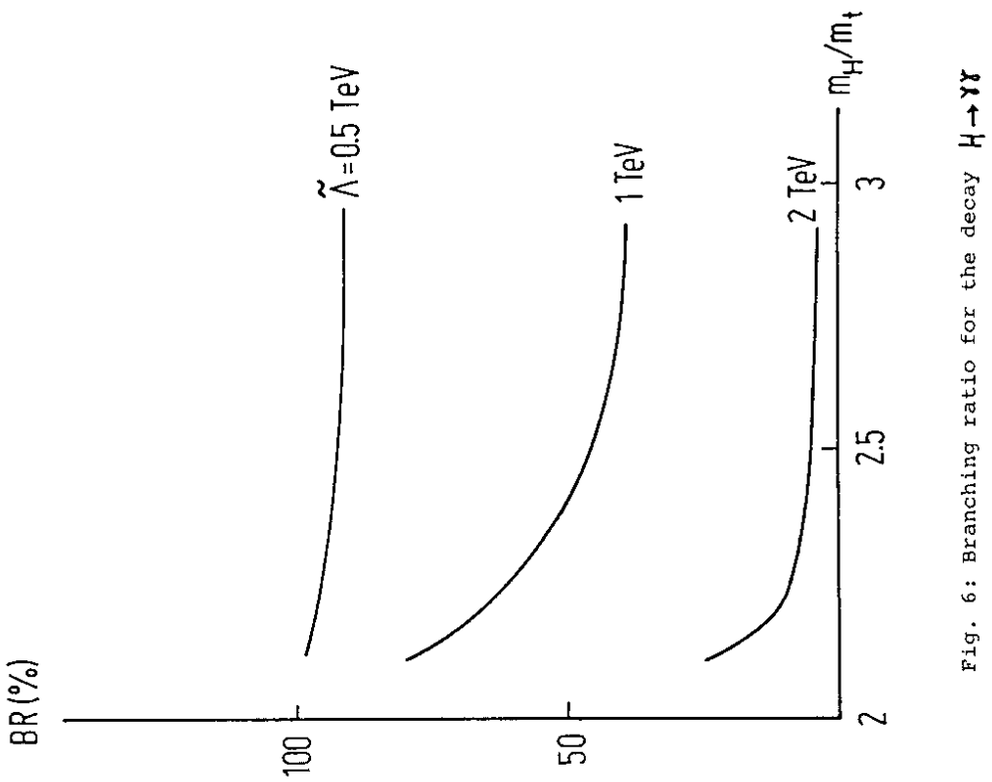

Fig. 6: Branching ratio for the decay $H \to \gamma\gamma$

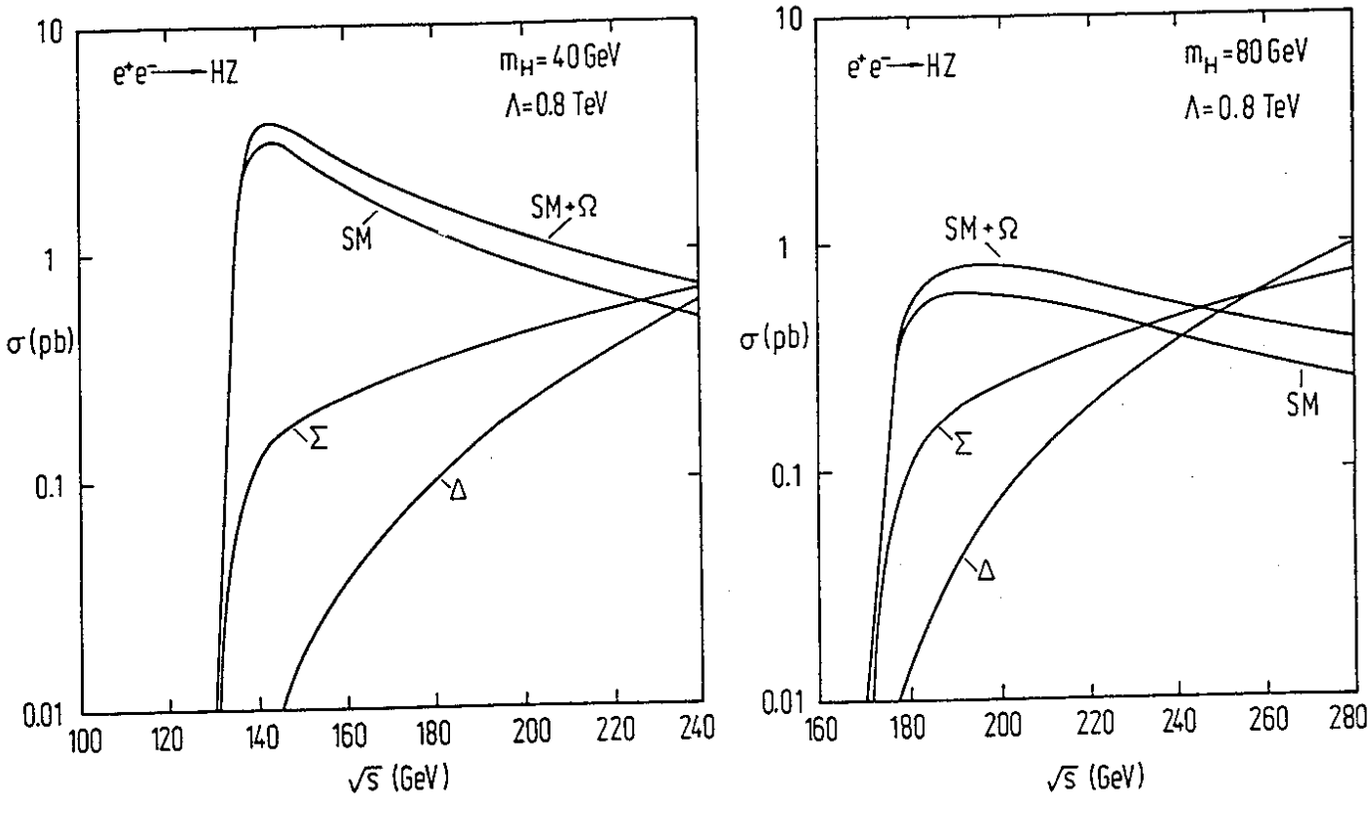

Fig. 4: Various cross sections for $e^+e^- \to HZ$ as explained in the text. Note that the exotic contributions win a factor of 16(!), if one goes to Λ=0.4 TeV.

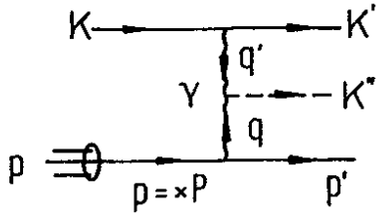

Fig. 7: Higgs production in ep collisions induced by the operator Ω

Fig. 8: Weizsäcker-Williams diagram for the process of fig. 11

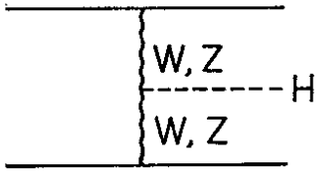

Fig. 9: Higgs production via vector boson fusion

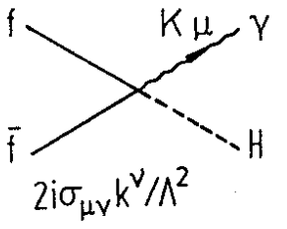

Fig. 10: Feynmanrule for the operator Σ

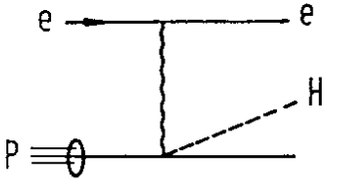

Fig. 11: Higgs production in ep collisions induced by the operator Σ

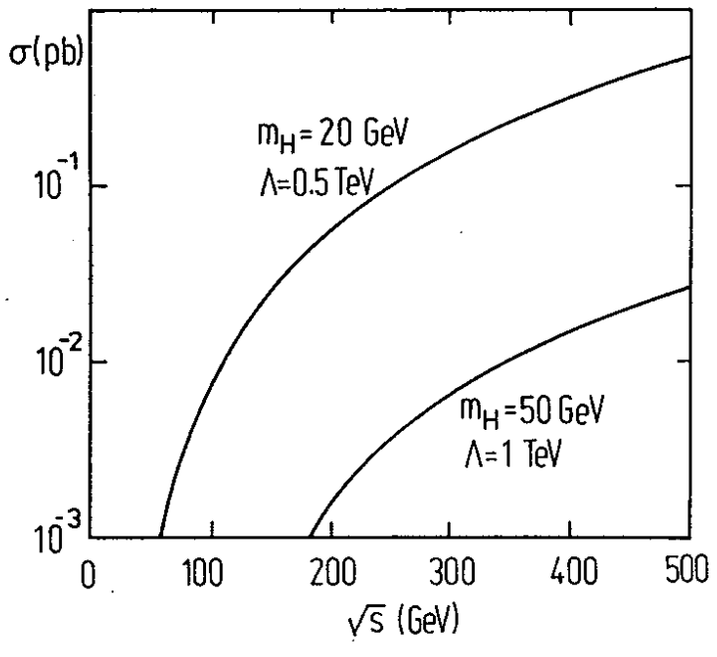

Fig. 12: Cross section for the process in fig. 11

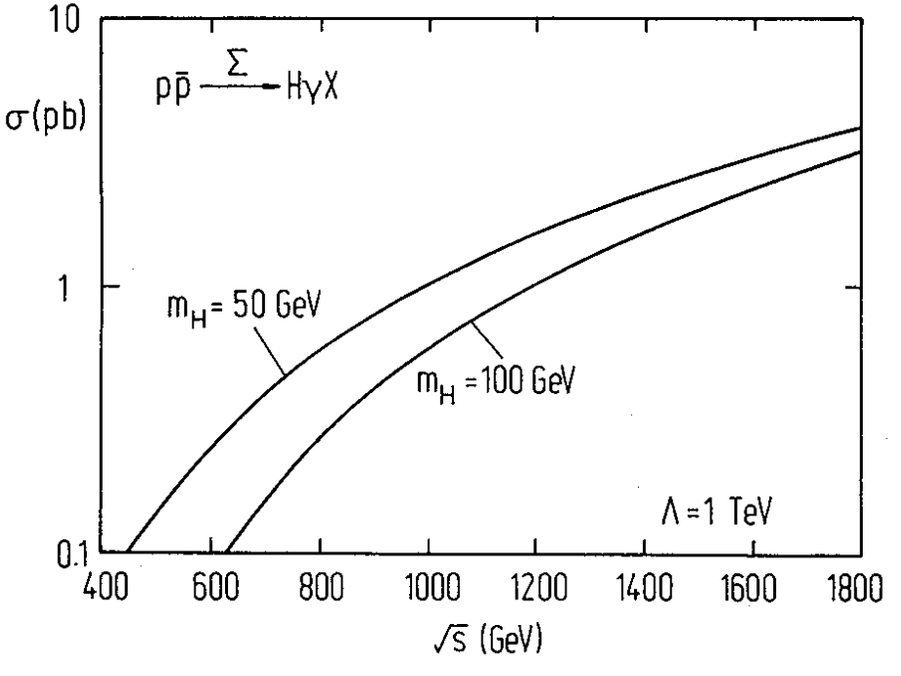

Fig. 13: Cross section for the production of the Higgs particle and a prompt photon in $p\bar{p}$ collisions, as induced by the operator Σ. Note that the cross section wins a factor of 16, if one goes to $\Lambda = 0.5$ TeV.

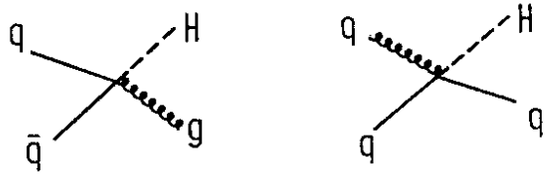

Fig. 14: Higgs+jet processes in $p\bar{p}$ collisions induced by the operator Σ

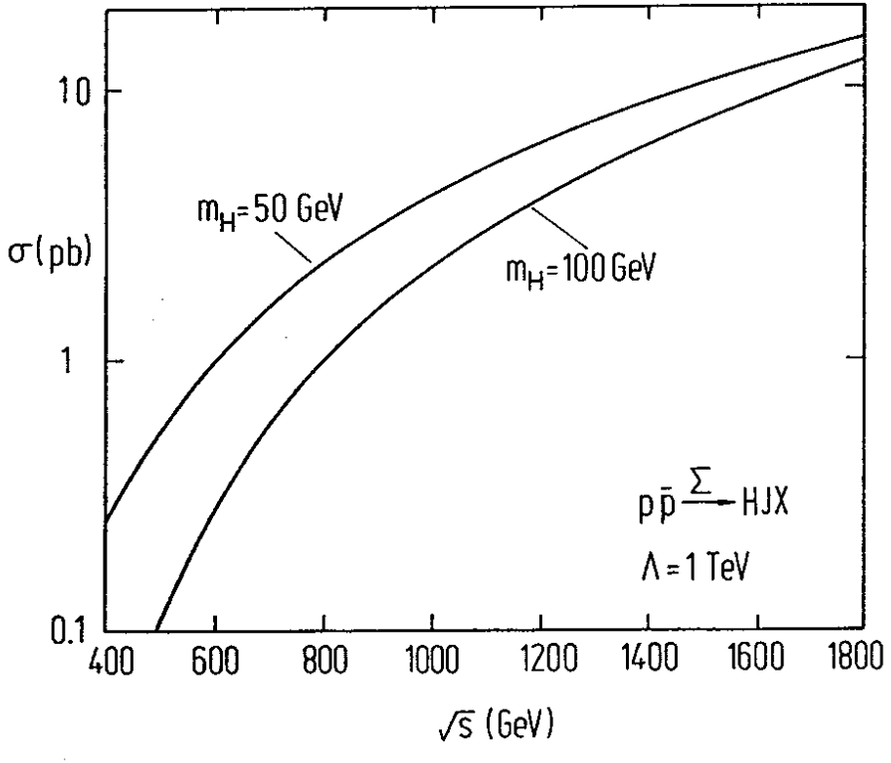

Fig. 15: Cross section for the production of the Higgs particle and a jet in $p\bar{p}$ collisions as induced by the operator Σ

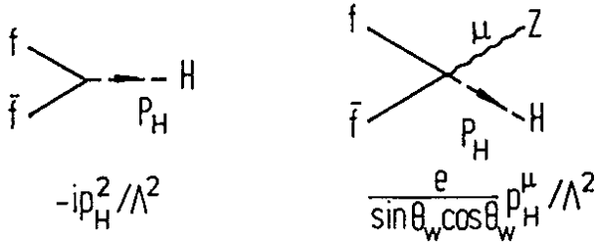

Fig. 16: Feynmanrules for the operator Δ

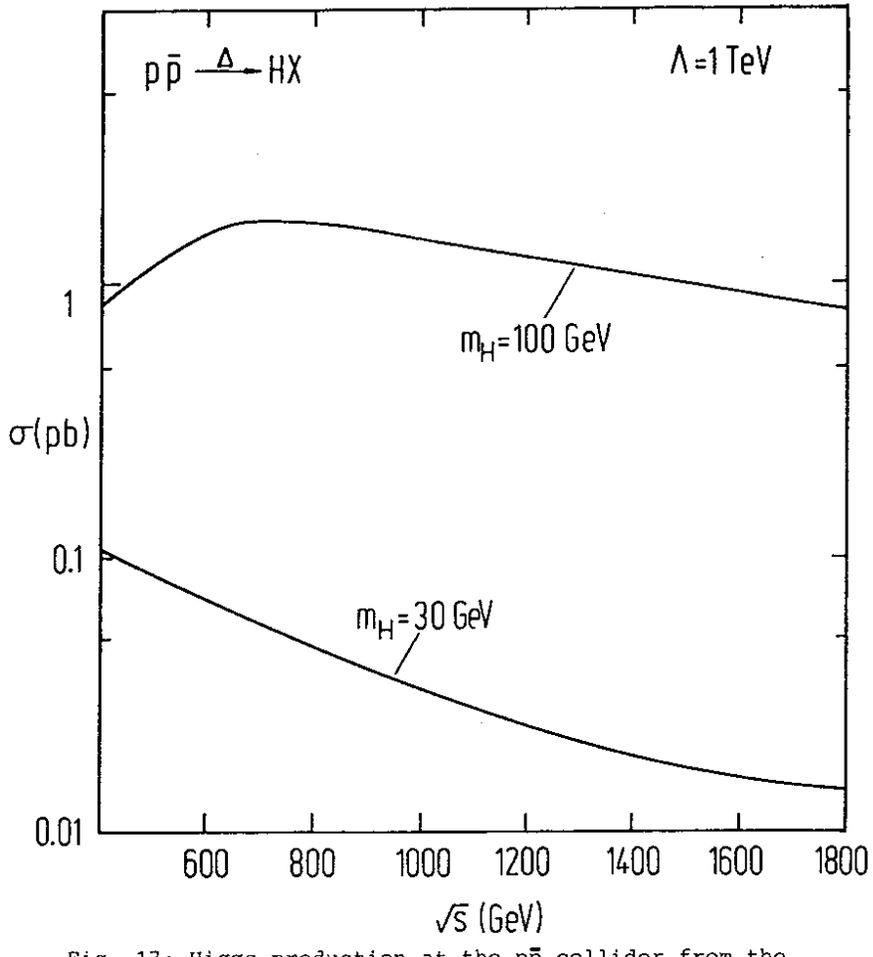

Fig. 17: Higgs production at the $p\bar{p}$ collider from the operator Δ for Λ=1 TeV and two values of the Higgs mass

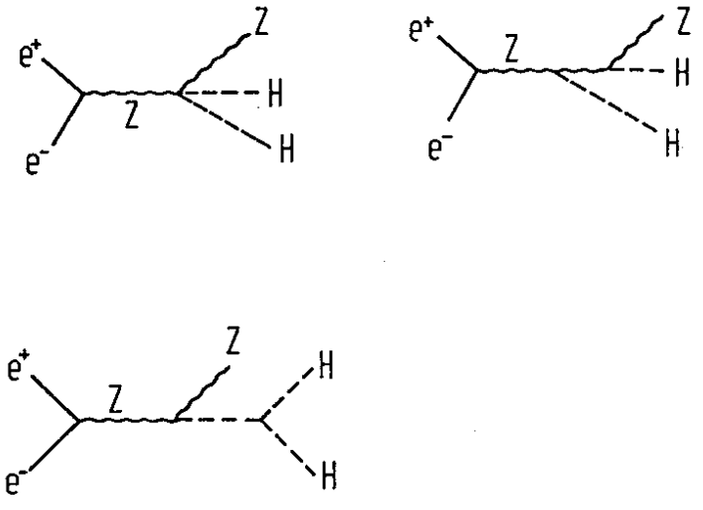

Fig. 18: Standard model mechanism for the production of two Higgs particles in e^+e^- annihilation

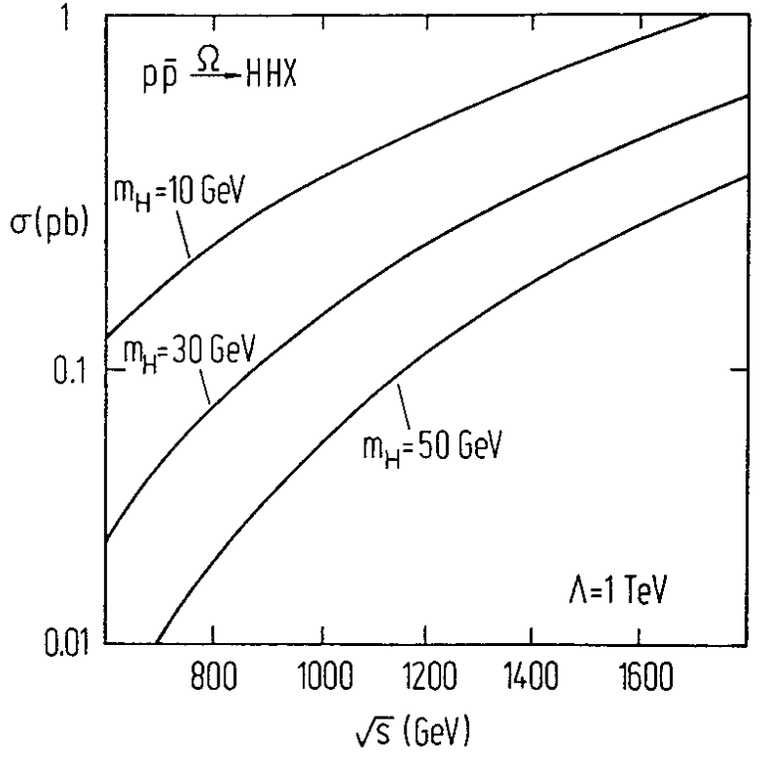

Fig. 19: Cross section for Higgs pair production by gg fusion in $p\bar{p}$ collisions